

Self-consistent first-principles calculations based on the embedded atomic sphere method

T. Komine and K. Shiiki

Department of Instrumentation Engineering, Keio University, Yokohama 223-8522, Japan

(Received 16 June 1999; revised manuscript received 1 November 1999)

We present a self-consistent embedded atomic sphere method. The embedded atomic sphere method is linearized for the easy calculation of wave functions. The coefficients of linearized basis sets inside spheres are determined to satisfy the continuity of the logarithmic derivatives between the inside and the outside of the sphere. We have applied this method to the hydrogen atom. It is shown that the calculated energy converges as the ratio of the sphere radius to the grid spacing increases. We implemented a self-consistent calculation for analysis of fcc hydrogen and the H_2 molecule. The calculated density of states of fcc hydrogen and the equilibrium interatomic distance of the H_2 molecule were found to be in good agreement with the results of conventional methods.

I. INTRODUCTION

In the past two decades, nonperiodic systems, such as surfaces, interfaces, and thin films, have attracted a great amount of attention from the viewpoints of nanoscale devices and microscopic material design. These systems show different properties from bulk materials. In these systems, quantum mechanical effects play an important role. Thus, in these systems in-depth knowledge of the electronic structure is of great scientific and technological importance. The peculiar characteristics of surfaces can be derived from the lack of symmetry or from a decrease in the number of neighboring atoms. Some authors have formulated the Green's function approach for treating infinite systems such as surfaces.¹

In recent years, approaches to electronic structure calculations with a real-space basis have been reported by some authors,²⁻⁴ a few of which utilize the finite difference (FD) in real space to achieve the linear-size scaling method or the order N method. These methods can exclude the restriction of periodicity and allow flexibility in the treatment of various boundary conditions and the realization of large-scale calculations. However, a large number of dense grids is necessary to calculate the electronic structure of transition metal systems even if pseudopotentials and curvilinear coordinates are used.⁵

Thijssen and Inglesfield proposed electronic structure calculation in real space for transition metal systems.⁶ Atomic spheres are embedded into the finite difference grids. However, it is difficult to solve the wave functions because of the use of energy-dependent basis sets in the atomic sphere, preventing the implementation of a self-consistent first-principles calculation. Moreover, they proposed a zero-derivative basis set to avoid the ambiguities regarding degeneracy.⁷ However, more than 100 basis sets were needed to obtain satisfactory results, and calculating these basis sets can be very time consuming.

In this paper, we first introduce the linearization of energy for the base inside the sphere and its connection condition in order to overcome the difficulties of solution of the wave functions, which includes the constraint minimization technique that is often used in pseudopotential calculations.⁸ Second, we solve the Poisson equation using a pseudocharge

distribution for the embedded atomic sphere in the FD grids. A self-consistent calculation can be implemented with the resulting effective potential. Last we apply this method to fcc hydrogen and H_2 and implement the self-consistent calculation.

II. METHODOLOGY

A. Linearized embedded atomic sphere method

Consider the calculation region as shown in Fig. 1(a). The calculation region is divided into uniform grids. The potential for the transition metals is very deep around the atomic core region even if a pseudopotential and curvilinear coordinates are used,⁵ and wave functions vary rapidly. It is pointed out that the grid points must be dense enough to obtain an exact solution, which requires large calculation power. In order to reduce the number of grid points, Thijssen and Inglesfield proposed that the grids inside the core region, where the potential rapidly varies, be replaced by an atomic sphere with radius R . Wave functions $\psi(\mathbf{r})$ inside the atomic spheres n are solved using a numerical technique based on a linear combination of radial functions of energy E in the original method.

Outside the spheres, the Kohn-Sham equation is approximated by the following finite difference equation:

$$\sum_{m=-1}^1 C_m [\psi(\mathbf{r}_p + m d \hat{\mathbf{i}}) + \psi(\mathbf{r}_p + m d \hat{\mathbf{j}}) + \psi(\mathbf{r}_p + m d \hat{\mathbf{k}})] + v_{\text{eff}}(\mathbf{r}_p) \psi(\mathbf{r}_p) - \epsilon \psi(\mathbf{r}_p) = 0, \quad (1)$$

where v_{eff} is the effective potential of the Kohn-Sham equation, \mathbf{r}_p indicates the grid point, d is the spacing of the grid, and $\hat{\mathbf{i}}, \hat{\mathbf{j}}, \hat{\mathbf{k}}$ are the unit vectors along the x, y, z directions. C_m is the expansion coefficient of the Laplacian, where $C_{\pm 1} = -1/d^2$ and $C_0 = 2/d^2$ for uniform grids.

A connection condition between inside and outside the sphere was proposed by Thijssen and Inglesfield.⁶ Briefly, their method utilized a radial function of energy E inside the sphere. A link across the sphere surface was considered as shown in Fig. 1(b), where \mathbf{r}_p^- and \mathbf{r}_a indicate the grid point vectors just outside and just inside the sphere, respectively.

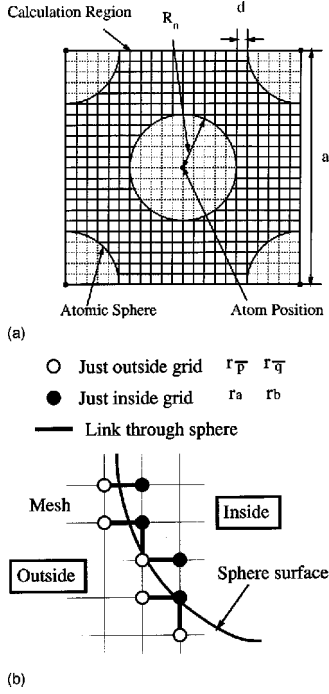


FIG. 1. (a) The embedded atomic spheres in the finite difference grid. The grid spacing is d and the radius of the atomic sphere n is R_n . (b) The links across the sphere's surface. The closed circles and open circles indicate the grids inside and outside the sphere, respectively. The bold lines are the links through the sphere's surface.

The pseudo-inner-product (PIP) between two functions $f(\mathbf{r})$ and $g(\mathbf{r})$ is defined as follows:

$$\langle f|g \rangle_B \equiv \sum_{(p,a)} f(\mathbf{r}_{\bar{p}})g(\mathbf{r}_a), \quad (2)$$

where (\bar{p},a) is the link through the sphere's surface as shown in Fig. 1(b). First, the matrix $S_{LL'}^{(n)}(E)$ was constructed from the PIP of the energy-dependent basis sets $\chi_{nL}(r_n, E)$. The coefficients of the basis sets were determined by multiplying the PIP between the energy-dependent basis inside and the trial function outside the sphere by the inverse of the matrix $S_{LL'}^{(n)}(E)$. Since the energy for the radial function must equal the eigenenergy, this energy was iteratively determined, requiring a loop to determine the eigenenergy. This method generated difficulties of degeneracy ambiguities. This energy searching requires great calculation time, while this energy dependence constitutes a challenge in implementing a self-consistent calculation. Thus, it is necessary that the additional energy loop should be removed to determine the eigenenergy and to implement a self-consistent calculation.

We expand the radial function $\chi_{nL}(r_n, E)$ for the energy parameter E_{nL} as $\chi_{nL}(r_n, E) \approx \chi_{nL}(r_n, E_{nL}) + (E - E_{nL})\dot{\chi}_{nL}(r_n, E_{nL})$, where L stands for the index (l, m) of the harmonics expansion and $\dot{\chi}_{nL}(r_n, E_{nL})$ is the energy derivative of the radial function $\chi_{nL}(r_n, E_{nL})$.⁹ Thus, the wave function only inside the atomic sphere n is

$$\begin{aligned} \psi(\mathbf{r}) &= \sum_L [a_{nL}\chi_{nL}(r_n, E_{nL}) + b_{nL}\dot{\chi}_{nL}(r_n, E_{nL})]Y_L(\hat{\mathbf{r}}_n) \\ &\equiv \sum_L [a_{nL}\phi_{nL}(\mathbf{r}, E_{nL}) + b_{nL}\dot{\phi}_{nL}(\mathbf{r}, E_{nL})] \end{aligned} \quad (3)$$

where $\mathbf{r}_n = \mathbf{r} - \mathbf{R}_n$, \mathbf{R}_n is the position of the atom n .

We proposed a different connection condition to determine the coefficients of the radial function in order to remove the additional energy loop. We expand the key idea and generate the energy-independent PIP,

$$\mathbf{S}^{(n)} \equiv \begin{bmatrix} S_{LL'}^{(n)} & S_{LL'}^{(n)} \\ S_{LL'}^{(n)} & S_{LL'}^{(n)} \end{bmatrix}, \quad (4)$$

and

$$S_{LL'}^{(n)} \equiv \sum_{(p,a)} \phi_{nL}(\mathbf{r}_{\bar{p}}, E_{nL})\phi_{nL'}(\mathbf{r}_a, E_{nL}),$$

$$S_{LL'}^{(n)} \equiv \sum_{(p,a)} \dot{\phi}_{nL}(\mathbf{r}_{\bar{p}}, E_{nL})\phi_{nL'}(\mathbf{r}_a, E_{nL}),$$

$$S_{LL'}^{(n)} \equiv \sum_{(p,a)} \dot{\phi}_{nL}(\mathbf{r}_{\bar{p}}, E_{nL})\dot{\phi}_{nL'}(\mathbf{r}_a, E_{nL}).$$

If the vectors

$$\mathbf{C}^{(n)} = [\dots, a_{nL}, \dots, b_{nL}, \dots]^T \quad (5)$$

and

$$\mathbf{P}^{(n)} = [\dots, \langle \psi | \phi_{nl'm'} \rangle_B, \dots, \langle \psi | \dot{\phi}_{nl'm'} \rangle_B, \dots]^T \quad (6)$$

are defined, the coefficients of the basis $\phi_{nL}, \dot{\phi}_{nL}$ can be calculated using the inverse of the energy-independent PIP,

$$\mathbf{C}^{(n)} = \mathbf{S}^{(n)-1}\mathbf{P}^{(n)}. \quad (7)$$

This operation includes the following: (i) the trial function on the grids is decomposed into components of each angular momentum, and (ii) two radial functions with the same angular momentum χ_{nL} and $\dot{\chi}_{nL}$ are weighted to satisfy the continuity condition. On the solution of the wave function, from Eq. (7) the coefficients of basis sets inside the spheres are obtained for a proper trial function such as the atomic wave function. As a result, the wave function inside the sphere and Eq. (1) can be calculated. In this study, the constraint minimization technique, which is often used in pseudopotential calculations, is utilized to solve the wave functions and eigenenergies.⁸ Consider the Hamiltonian operation of Eq. (1) to the grid $\mathbf{r}_{\bar{p}}$ just outside the sphere. This operation is partly written as

$$\dots + \frac{2}{d^2}\psi(\mathbf{r}_{\bar{p}}) - \frac{1}{d^2}\psi(\mathbf{r}_a) + v_{\text{eff}}(\mathbf{r}_{\bar{p}})\psi(\mathbf{r}_{\bar{p}}) = \epsilon\psi(\mathbf{r}_{\bar{p}}). \quad (8)$$

Since the wave function inside the sphere $\psi(\mathbf{r}_a)$ is

$$\begin{aligned}
\psi(\mathbf{r}_a) &= \sum_L [a_{nL}\phi_{nL}(\mathbf{r}_a) + b_{nL}\dot{\phi}_{nL}(\mathbf{r}_a)] \\
&= [\dots, \phi_{nL}(\mathbf{r}_a), \dots, \dot{\phi}_{nL}(\mathbf{r}_a), \dots] \times \mathbf{S}^{(n)-1} \\
&\times \left[\dots, \sum_{(\bar{q},b)} \psi(\mathbf{r}_{\bar{q}})\phi_{nL'}(\mathbf{r}_b), \dots, \sum_{(\bar{q},b)} \psi(\mathbf{r}_{\bar{q}}) \right. \\
&\quad \left. \times \dot{\phi}_{nL'}(\mathbf{r}_b), \dots \right]^T, \tag{9}
\end{aligned}$$

the left-hand side of Eq. (8) is energy independent, where (\bar{q}, b) is the link through the sphere's surface. On the other hand, the relation between grids just outside is energy dependent when the same Hamiltonian operation is considered. This energy-independent relation enables one to utilize an iterative minimization and to easily perform the orthogonalization.

B. Self-consistent calculation

Our aim is to develop a self-consistent calculation method for nonperiodic systems. In general, the potential inside the sphere can be formulated as a boundary value problem using a Green's function,¹⁰

$$v_c(\mathbf{r}) = \int_{S_n} \rho(\mathbf{r}') G(\mathbf{r}_n, \mathbf{r}') d\mathbf{r}'_n - \frac{R_n^2}{4\pi} \oint_{S_n} v_c(\xi'_n) \frac{\partial G}{\partial r'_n} d\Omega'_n, \tag{10}$$

where ξ'_n is a point on the sphere n and R_n is the radius of the sphere n . The Green's function G satisfies the equations

$$\begin{aligned}
\nabla^2 G(\mathbf{r}_n, \mathbf{r}'_n) &= -\delta(\mathbf{r} - \mathbf{r}'), \\
G(\mathbf{r}_n, \xi'_n) &= 0. \tag{11}
\end{aligned}$$

If the charge density everywhere and the boundary condition implied in the calculation region are given, the boundary value on the sphere can be calculated numerically. However, the charge density around the core region oscillates rapidly with higher frequencies than the resolution of the grid spacing d when a transition metal system is treated. If the core charge density is projected onto the grids, an accurate solution cannot be obtained. In this work, a pseudocharge density $\bar{\rho}(\mathbf{r})$ is introduced, which is smooth enough to calculate using the standard FD method without the use of dense grids.

The charge distribution $\rho(\mathbf{r})$ inside the sphere is given by the multipole expansion,

$$\rho(\mathbf{r}) = \sum_{lm} \rho_{nlm}(r_n) Y_{lm}(\hat{\mathbf{r}}_n). \tag{12}$$

The potential outside the sphere for the pseudocharge distribution is the same as for the real charge distribution if the pseudocharge inside has the same multipole moment as the real charge. Thus, the real radial charge density $\rho_{nlm}(r_n)$ inside the sphere n can be replaced by a pseudocharge $\bar{\rho}_{nlm}(r_n)$ having the same multipole moment,

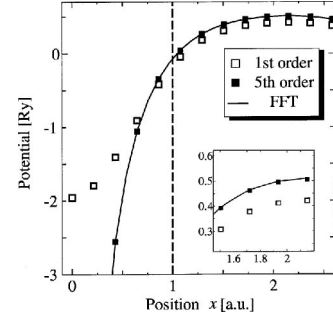


FIG. 2. The solution of the Poisson equation for the fcc hydrogen nucleus. The solid line indicates the potential of the real charge density with the FFT scheme. The open and closed squares show the potentials of the pseudocharge density with the FD scheme, which are replaced by a linear function and a fifth order polynomial. The dashed horizontal line indicates the sphere's surface with a radius of 1.0 a.u.

$$\int_0^{R_n} r^l \rho_{nlm}(r_n) r_n^2 dr_n = \int_0^{R_n} r^l \bar{\rho}_{nlm}(r_n) r_n^2 dr_n. \tag{13}$$

In this work, the pseudocharge is represented by a polynomial function, which equals the real charge in the multipole moment and matches the value on the sphere boundary and its n th derivatives.

The Coulomb potential in the whole region is calculated by numerically solving the Poisson equation with the standard FD in the appropriate boundary condition. The potential on the whole region of space is obtained when the boundary value is given by interpolation from the potential on the grid points.

The adequacy of the introduced pseudocharge is verified for solution of the Poisson equation. The potential only outside the sphere is needed when the Poisson equation is solved using the FD method. So, at least the outside potential for the pseudocharge density must agree with that for the real charge. For the fcc hydrogen ion, two potentials are calculated using the FD method, where the lattice constant a is 4.3 a.u. and the sphere radius R is 1.0 a.u. Figure 2 shows the potential of the pseudocharge using the FD approach and the potential of the real charge calculated by a fast Fourier transform (FFT) scheme with a cutoff energy of 500 Ry. The degrees of the polynomial for the pseudocharge are 1 or 5 in Fig. 2. It is clearly found that the outside potential of the pseudocharge density is in excellent agreement with that of the real charge density.

III. APPLICATION

We apply the linearized embedded atomic sphere method to the hydrogen atom without self-consistent calculation in order to investigate the effect of linearization. This problem is modeled by a hydrogen atom positioned in the center of a cubic region having a side of 30 a.u. The boundary condition is that wave functions are forced to be zero at the edge of the calculation region. This length of 30 a.u. is small enough to calculate wave functions for the principal number $n=1$ with negligible influence from the calculation region. When the energy parameter is shifted from the exact eigenvalue -1.0 Ry, the calculated energies are shown in Fig. 3. Since

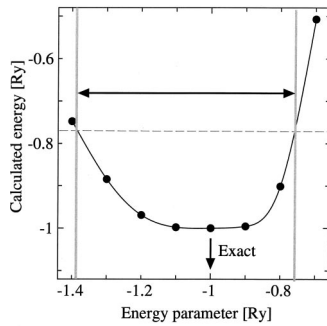


FIG. 3. Calculated eigenvalues from one self-consistent iteration for various energy parameters around an exact eigenvalue -1.0 Ry for the principal number $n=1$. The vertical gray lines indicate the maximum permissible range to obtain the exact eigenvalue after self-consistent iterations.

the energy parameters are also calculated with self-consistent procedures, the energy parameters of the next step should be closer to the exact eigenvalue.

The accuracy of the eigenvalues in this method is changed by varying the grid spacing d and the sphere radius R . The smaller the grid spacing, the more the eigenvalue approaches a constant value. In this method, the calculated eigenvalue also depends on the sphere radius in addition to depending on the grid spacing. So a quantity Q is defined as $Q=R/d$. Suppose that the calculated eigenvalue for $R=5$ a.u. and $d=0.2$ a.u., which correspond to $Q=25$, is the standard value, and consider the difference between the calculated eigenvalue for various Q 's and the standard value. Figure 4 shows the energy difference dependence on the quantity Q for the hydrogen atom calculated using this method. The quantity Q is varied by changing the sphere radius R and the grid spacing d . The energy difference of the hydrogen atom converges as the quantity Q increases. The formalism of our method resembles the linearized augmented plane wave (LAPW) method except for the restriction of periodicity.⁹ The value RK_{\max} is known to be a standard quantity of the variation in the LAPW method. The accuracy of this method is thought to depend on the sphere radius and the grid spacing. The quantity corresponding to that of LAPW in this method is thought to be $Q=R/d$ through analogy.

We have implemented this method and tested it for fcc hydrogen. The unit cell is a simple cubic lattice consisting of four hydrogen atoms. The lattice constant is 4.3 a.u. The number of \mathbf{k} points in $1/48$ wedge of the Brillouin zone (BZ)

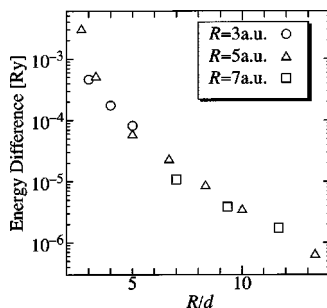


FIG. 4. The dependence of energy difference on the quantity $Q=R/d$. The open circles, the triangles, and the squares show $R=3.0, 5.0,$ and 7.0 a.u., respectively, on various grid spacings d .

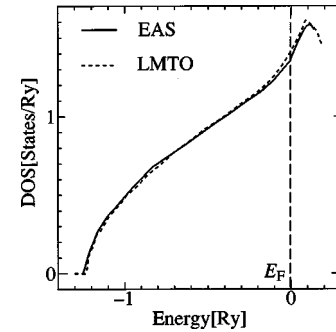


FIG. 5. Density of states for fcc hydrogen. Solid line and dotted line are calculated using this method (EAS) and the conventional method (LMTO), respectively.

is 35. A self-consistent calculation for the energy parameters and the total potential is implemented. In the original method, a loop to determine the eigenenergy was needed in addition to the self-consistent loop. In our method, energy parameters are determined on each self-consistent iteration from the center of the projected density of states in each angular momentum of each atomic sphere. Determination of the energy parameter was carried out at the same time using a self-consistent calculation. The initial guess for energy parameters is atomic levels of -1 Ry for the principal value of $n=1$. As the exchange-correlation potential, we employ that parametrized by Perdew and Zunger¹¹. For the wave function and the effective potential inside the sphere, the maximal angular momentum l is $l=2$. Though this value is smaller than that of the FLAPW method, the smaller sphere radius is favorable for this circumstance since the spherical component of $l=0$ is dominant near the core region. Figure 5 shows the density of states (DOS) calculated using this method and for comparison also shows that of the linear muffin-tin orbital (LMTO) method. The radius of the atomic sphere R is 1.0 a.u. and the grid spacing d is $a/20$. The calculated density of states of hydrogen is in good agreement with that arrived at using the conventional method. Such a satisfactory result cannot be obtained even if the same grid spacing is used in conjunction with the simple FD method.

We have also applied our approach to the hydrogen molecule H_2 as an example of a localized (nonperiodic) system. We used a cubic supercell with a size of 10 a.u. The grid spacing d and the atomic sphere radius R are 0.25 a.u. and 0.5 a.u., respectively. The sampling of \mathbf{k} points in the BZ is

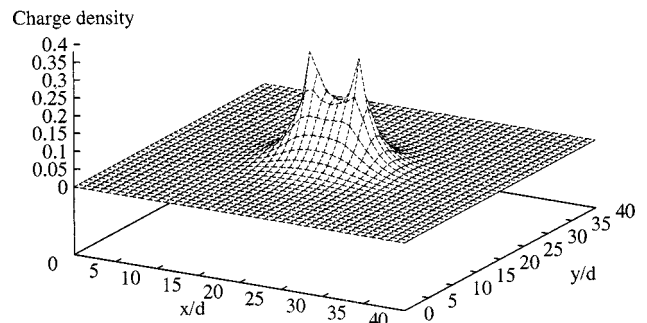


FIG. 6. Three-dimensional representation of charge density of the H_2 molecule with interatomic distance $d_{H-H}=1.44$ a.u. The cross section is a plane including two hydrogen atoms.

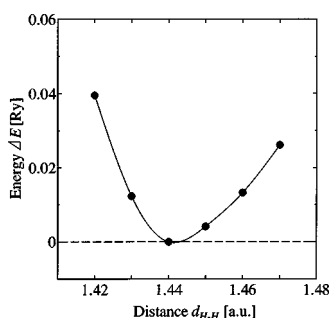


FIG. 7. Total energy of the H_2 molecule with various interatomic distances d_{H-H} . The energies ΔE are shown related to the standard value of total energy at a distance of 1.44 a.u.

only at the Γ point. The criterion for convergence is 10^{-6} Ry in the total energy. Figure 6 shows a three-dimensional representation of the charge density of the H_2 molecule with a distance d of 1.44 a.u. between hydrogen atoms. The covalent bond of the H_2 molecule is well reproduced using this method. Figure 7 shows the total energy as a function of interatomic distance. The standard value is the total energy for interatomic distance $d = 1.44$ a.u. The equilibrium interatomic distance is estimated to be about 1.44 a.u., which agrees with other local-density approximation results (1.44–1.45 a.u.).¹²

IV. CONCLUSIONS

We have developed a self-consistent embedded atomic sphere method of calculating electronic structure using a linearized radial function of energy, improving on the previous method. The linearized radial function leads to an energy-

independent relation among the grids and enables one to utilize iterative techniques of constraint minimization. On constructing the Coulomb potential, a pseudocharge inside the atomic sphere is introduced in order to treat the charge distribution oscillating near the core region. These techniques lead to easy implementation of the self-consistent calculation.

This method is applied to the hydrogen atom, demonstrating the ease with which wave functions can be calculated. The eigenenergy variationally converges as the ratio between the sphere radius R and grid spacing d increases. The method is applied also to fcc hydrogen and its efficiency is examined. The calculated density of states of hydrogen is in good agreement with that calculated by conventional methods. Our method requires a less dense grid than the finite difference method without the atomic sphere. For the H_2 molecule, the covalent bond and the equilibrium interatomic distance agree with those arrived at by other calculations.

This method has the advantages of both finite difference and atomic sphere. The former can easily combine with any boundary condition such as Dirichlet and Neumann, which is important for calculating a nonperiodic system. The latter allows one to treat systems including transition metals. This method does not have the restriction of the periodicity of a wave function and has the advantage of being essentially full potential, thus allowing the study of nanoscale devices using appropriate boundary conditions.

ACKNOWLEDGMENTS

We are grateful to J. M. Thijssen and T. Kai for their fruitful comments. We wish to thank the Supercomputer Center, Institute of Solid State Physics, University of Tokyo, for technical support.

¹See, for example, W. Kohn, Phys. Rev. B **11**, 3756 (1975); H. L. Skriver and N. M. Rosengaard, Phys. Rev. B **43**, 9538 (1991).

²A. Devenyi, K. Cho, T. A. Arias, and J. D. Joannopoulos, Phys. Rev. B **49**, 13 373 (1994).

³J. R. Chelikowsky, N. Troullier, K. Wu, and Y. Saad, Phys. Rev. B **50**, 11 355 (1994).

⁴T. Hoshi, M. Arai, and T. Fujiwara, Phys. Rev. B **52**, R5459 (1995).

⁵N. A. Modine, G. Zumbach, and E. Kaxiras, Phys. Rev. B **55**, 10 289 (1997).

⁶J. M. Thijssen and J. E. Inglesfield, Europhys. Lett. **27**, 65 (1994).

⁷J. M. Thijssen and J. E. Inglesfield, Phys. Rev. B **51**, 17 988 (1995).

⁸M. C. Payne, M. P. Teter, D. C. Allan, T. A. Arias, and J. D. Joannopoulos, Rev. Mod. Phys. **64**, 1045 (1992).

⁹O. K. Andersen, Phys. Rev. B **12**, 3060 (1975).

¹⁰M. Weinert, J. Math. Phys. **22**, 2433 (1981).

¹¹J. P. Perdew and A. Zunger, Phys. Rev. B **23**, 5048 (1981).

¹²R. M. Dreizler and E. K. U. Gross, *Density Functional Theory* (Springer-Verlag, Berlin, 1990).